Progress In Electromagnetics Research B, Vol. 18, 149–163, 2009

TRANSPARENT SHELLS — INVISIBLE TO ELECTROMAGNETIC WAVES

Z. L. Mei † and T. J. Cui

State Key Laboratory of MillimeterWaves
Department of Radio Engineering
Southeast University
2 Sipailou Road, Nanjing 210096, China

Abstract—In this paper, we study metamaterial-based transparent shells, which are invisible to electromagnetic waves and fields. More general topics, including material loss, material discretization and far field distribution etc. are covered in order to facilitate possible realization. We design and analyze the transparent shells using optical transformation. Unlike the widely-studied cloaking devices which make the objects inside invisible, the transparent shells physically cover and shield the devices inside without sacrifice of their electrical performance since they are transparent to incoming electromagnetic waves. Due to the simple constitutive parameters, these transparent structures could be realized using artificial metamaterials in a wide frequency band, which may have wide applications in civil and military areas.

1. INTRODUCTION

Invisible cloaks are deliberately designed electromagnetic shielding structures which make the shielded objects invisible to the outside world. By introducing the powerful tools of optical transformation, Pendry et al. theoretically predicted the existence of invisible cloaks [1]. A few months later, the laboratory prototype of the cloak was experimentally verified [2]. Since then, various cloaks are designed, theoretically proved, and simulated with different methods [3–16]. Pursue for invisible cloaks near the optical frequency is also under consideration and they are experimentally demonstrated very recently [17–21]. Using the same idea, other fabulous microwave

Corresponding author: Z. L. Mei (meizl@lzu.edu.cn).
† Also with School of Information Science and Engineering, Lanzhou University, 222 South Tianshui Road, Lanzhou 730000, China.

devices like inside-out cloaks, rotators, concentrators, antennae, and reflectionless waveguide bends have also been designed and verified [22–32]. Recently, the finite embedded coordinate transformation is proposed [33], another technology to transmute the singularities is also demonstrated theoretically and experimentally [34, 35].

Actually, cloaking devices can also be realized by other methods. In this regard, Alù and Engheta have proposed the scheme of scattering cancellation, in which dipole moments created by an object is cancelled by covering it with a plasmonic or a metamaterial coating [36, 37]. The mechanism has been shown to have potential applications in a wide range of areas [38, 39]. Anomalous localized resonance has also been utilized to conceal small objects, and the cloaking can be achieved in the region external to the cloak [40]. Very recently, a broadband exterior cloaking mechanism, which is based on destructive interference using active cloaking devices, is also proposed by Milton and coworkers [41, 42]. In contrast to these methods, Tretyakov et al. theoretically and experimentally realized broadband cloaking devices by using transmission-line networks [43, 44]. All these developments will drastically expand the range of cloaking devices.

In our previous work, the concept of transparent cloaks is proposed and theoretically investigated using the optical transformation [6, 45]. In this paper, the previous work is further extended to cover more general topics, including general transformation function and geometry, material loss, layered homogeneous structure for possible realization and numerical calculation of the far field distribution etc. The correctness of the device is also theoretically proved. And more full-wave simulations are given to validate the results. Compared to the above-mentioned invisible cloaks, the proposed shell structures are transparent to electromagnetic fields, implying that electromagnetic waves can penetrate the shells and interact with the devices inside as if the shells do not exist. The reversed process is also valid. For radiators inside the transparent shells, the radiated fields are unaffected inside and outside the structures. Hence, the transparent shells may have wide applications in the radome structures for antennae and radar stations, in the design of materials for protecting electronic equipments, and in the construction of anechoic rooms and concert halls, etc. The results complement our previous study and they together provide a more complete understanding for the new devices. We notice that Kwon et al. use similar idea in their design for antennae in complex scattering environments, however, they focus on its applications [3]. In contrast to their work, we pay much more attention to the detailed design process.

2. THEORETICAL ANALYSIS

When using the optical transformation, two spaces are usually considered, i.e., the virtual space and the transformed physical space. In most cases, part of the virtual space is mapped to the physical space by a general coordinate transformation. Based on the covariance of Maxwell's equations, the mapping can be interpreted as the change of material parameters in the same region. Hence, the physical implementation of the newly-created 'materials' in the transformed space can be considered as new devices, which may have fabulous properties due to the specific transformation. However, the theories behind are equivalent to those in the original virtual space [46–48]. Suppose that the original and physical spaces are represented by xyz and $x'y'z'$, respectively. Then, with a general coordinate transformation, the resulting material parameters are as follows

$$\epsilon' = \mu' = \mathsf{A}\epsilon\mathsf{A}^{\mathsf{T}}/\mathtt{det}\mathsf{A}, \tag{1}$$

in which A is the Jacobian matrix between the two spaces. And

$$\mathsf{A} = \frac{\partial(x', y', z')}{\partial(x, y, z)} = \begin{bmatrix} \frac{\partial x'}{\partial x} & \frac{\partial x'}{\partial y} & \frac{\partial x'}{\partial z} \\ \frac{\partial y'}{\partial x} & \frac{\partial y'}{\partial y} & \frac{\partial y'}{\partial z} \\ \frac{\partial z'}{\partial x} & \frac{\partial z'}{\partial y} & \frac{\partial z'}{\partial z} \end{bmatrix}. \tag{2}$$

Imagine a complex-connected region in the virtual space, which has a 'hole' in the center. If a mapping is chosen as such that only the interior points in the region are changed but the boundary points are unchanged, then, according to the above theory, the resulting structure in the physical space is transparent to electromagnetic waves. Both fields inside and outside the structure are not affected as if the structure does not exist. This structure can be used as a transparent shell.

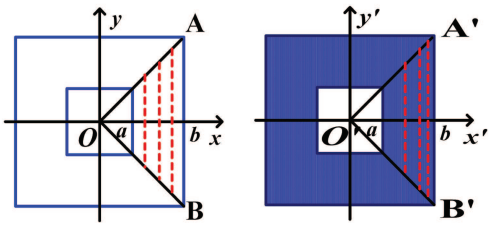

Figure 1. Virtual space (left) and the physical space (right) for the transparent shell.

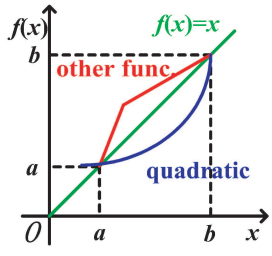

Figure 2. A few kinds of transformation functions for the transparent shell.

As an example, we design a square-shaped transparent shell, whose inner and outer widths are $2a$ and $2b$, respectively. Fig. 1 shows the coordinate transformation between the original space (vacuum) and the transformed space. Note that only one quarter of the region, i.e., the area OAB, is considered due to the symmetry of the structure. The transformation is chosen as

$$x' = f(x), \quad f(a) = a, \quad f(b) = b, \tag{3}$$

$$y'/x' = y/x, \tag{4}$$

$$z' = z. \tag{5}$$

Utilizing Eqs. (1)–(5), it is easy to get the material parameters in the physical space

$$\epsilon' = \mu' = \begin{bmatrix} r & s & 0 \\ s & (s^2+1)/r & 0 \\ 0 & 0 & r/(f')^2 \end{bmatrix}, \tag{6}$$

in which $r = f'x/x'$, $s = t(r-1)$, $t = y'/x'$, $f' = \mathrm{d}f/\mathrm{d}x$ and $x = f^{-1}(x')$.

Note that $f(x)$ is an arbitrary function passing through points (a, a) and (b,b), as shown in Fig. 2. Hence, we have freedom to simplify the material parameters and optimize the structure. The polynomial form for $f(x)$ is

$$f(x) = (x-a)(x-b)g(x) + x, \tag{7}$$

where $g(x)$ is a polynomial function of x. When $g(x) = 0$, one gets the trivial mapping $x' = x$; let $g(x) = C$, the quadratic form is obtained and is used throughout the paper. If piecewise continuous functions are allowed, which is certainly sure for this case, one has more freedom to choose. Fig. 2 gives a few kinds of transformation functions.

Since both the permittivity and permeability tensors are symmetric matrices, they can be diagonalized. The result is as follows

$$\epsilon' = \begin{bmatrix} \epsilon_{xx} & 0 & 0 \\ 0 & \epsilon_{yy} & \\ 0 & 0 & \epsilon_{zz} \end{bmatrix} \tag{8}$$

where

$$\epsilon_{xx} = \left\{ S + \left[S^2 - 4r^2 \right]^{1/2} \right\} / (2r), \tag{9}$$

$$\epsilon_{yy} = \left\{ S - \left[S^2 - 4r^2 \right]^{1/2} \right\} / (2r), \tag{10}$$

$$\epsilon_{zz} = r / \left(f' \right)^2. \tag{11}$$

and $S = r^2 + s^2 + 1$.

The same results are valid for the permeability μ. Such formulas are important for the practical implementation of the transparent shells.

If the width of the inner square approaches zero, we get a square-shaped transparent post in the physical space with side length $2b$ instead of a hollow shell, which may find applications in anechoic rooms or concert halls.

Suppose that a TE-polarized plane wave is propagating in the virtual space, which can be represented as

$$E_z = E_0 \exp\left[-\mathtt{j}\left(k_x x + k_y y\right)\right], \tag{12}$$

$$H_x = H_{x0} \exp\left[-\mathtt{j}\left(k_x x + k_y y\right)\right], \tag{13}$$

$$H_y = H_{y0} \exp\left[-\mathtt{j}\left(k_x x + k_y y\right)\right]. \tag{14}$$

For regions inside and outside the shell in the transformed space, the fields are the same as those in the virtual space. While for the shell itself, fields can be expressed using the following equations [46–48].

$$\mathbf{E}' = (\mathsf{A}^{-1})^{\mathsf{T}}\mathbf{E}, \quad \mathbf{H}' = (\mathsf{A}^{-1})^{\mathsf{T}}\mathbf{H}. \tag{15}$$

Through simple algebraic manipulation, one has the following expressions at $x = a$,

$$E'_z|_{x=a^-} = E'_z|_{x=a^+}, \tag{16}$$

$$H'_y|_{x=a^-} = a/f(a)H_y = H'_y|_{x=a^+}. \tag{17}$$

Similar results can be obtained at $x = b$ and other boundaries. The continuity of the tangential fields at the two boundaries is clearly shown, which verifies the correctness for the process. This result holds for both TE and TM waves because of the principle of superposition and duality.

Actually, same ideas can be exploited to design the transparent structures in one-dimensional and three-dimensional situations, and transparent shells with more complicated and even arbitrary shapes can also be envisioned.

3. NUMERICAL RESULTS AND DISCUSSION

To further validate the proposed transparent structures, full-wave simulations are conducted using the finite-element based software, COMSOL Multiphysics. In all simulations, material parameters for the transparent shell are set according to Eq. (6). The space inside and outside the shell are considered as air, and all structures are surrounded by PML layers. Fig. 3 shows the field distribution of the square-shaped transparent shell under the incidence of plane waves. When the incident waves hit the shell, no backward reflections and

scattering happen, and the 'shadowed' region is absent too, which is an intrinsic property under the optical transformation. The fields are distorted in the shell according to Eq. (15). While for regions inside and outside the shell, fields restore to its original form as if the structure does not exist. Thus we conclude that the proposed transparent structure can actually protect things inside while does not affect their electromagnetic performance at all.

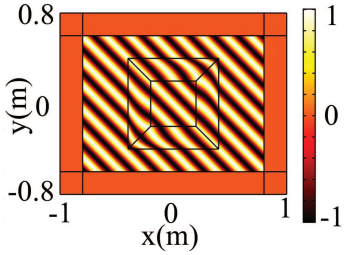

Figure 3. The electric-field distribution of the square-shaped transparent shell under the plane-wave incidence, in which $a = 0.2\,\mathrm{m}$, $b = 0.4\,\mathrm{m}$, and the frequency is $2\,\mathrm{GHz}$. Here, the transformation function is $f(x) = -2.5(x - 0.5)^2 + 0.425$.

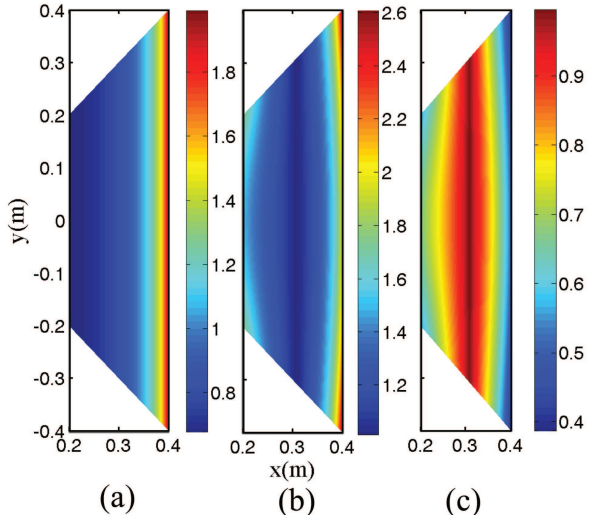

Figure 4. Electromagnetic parameter distributions for the proposed transparent structure. (a) The ϵ_{zz} component. (b) The μ_{xx} component. (c) The μ_{yy} component.

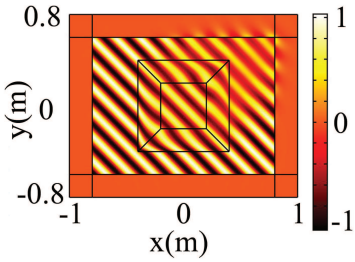

Figure 5. The full-wave simulation results for the square transparent shell with electric and magnetic-loss tangents of 0.05. Other parameters are the same as those in Fig. 3

Material parameters for the proposed transparent shell are given in Fig. 4. For the incidence of TE-polarized wave, only three parameters, ϵ_{zz}, μ_{xx}, and μ_{yy} are relevant, as shown in Fig. 4. It is clear that no singular values are present, and the range of the parameters is feasible for real implementation. We can see that the ϵ_{zz} component varies from 0.6 to 2.0 approximately, while the ranges for μ_{xx} and μ_{yy} are 1.0 to 2.6 and 0.4 to 1.0 respectively. All parameters can be realized using the artificial metamaterials.

We remark that we only choose the quadratic form for the transformation function arbitrarily. Higher-order functions may ease the practical implementation further when the material constraints are taken into consideration, like those shown in [18]. Further researches on this area are under consideration.

When metamaterials are used for practical implementation of the transparent shell, one has to take the losses into consideration. In Fig. 5, the electric field distribution for the same transparent structure is demonstrated, which is designed with lossy materials having electric and magnetic loss tangent of 0.05. It is shown that the magnitude of the field gets smaller passing through the device due to the material loss, and a shadow is cast behind the device, however, the shape of the phase front is kept very well and no reflection is observed. Fig. 5 thus confirms the practical realization and application for the proposed device.

Another problem is also unavoidable when real-world implementation is considered, i.e., the inhomogeneity. This can be easily solved by using layered homogeneous materials. The simulation results are given in Fig. 6. In Fig. 6, the square-shaped transparent shell in Fig. 3 is divided into 5, 10 and 20 layers respectively in order to show the performance dependance on layer numbers. The depth of the layer

thus corresponds to 4/15, 2/15 and 1/15 wavelengths respectively. For each layer, the material parameters are taken as those on the layer interfaces. Two incident angles are considered, 0 and 45 degree with respect to the x-axis direction. The magnitude of the incident plane wave is 1 V/m. Due to the discretization, their exists scattering field in all cases (note the magnitude of the electric field and the shape of

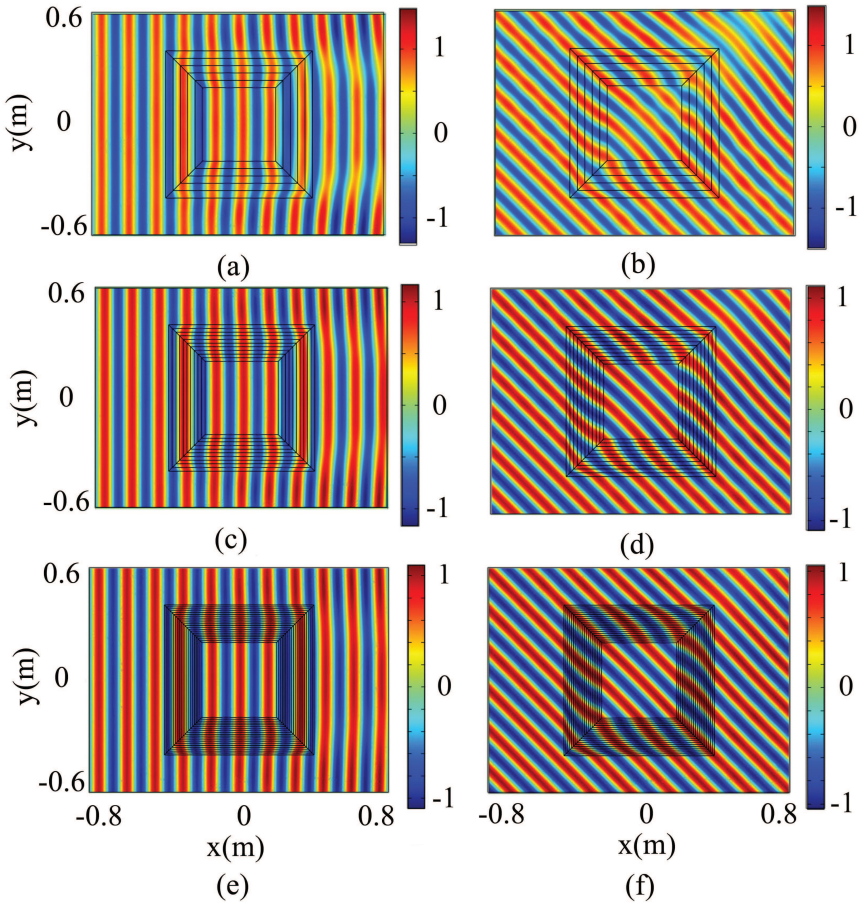

Figure 6. Electric field distribution for layered transparent shells. The geometry of the structure is the same as it in Fig. 3. The shell is divided into 5 (a) and (b), 10 (c) and (d) and 20 (e) and (f) layers respectively. The incident angle of the plane wave with respect to x-axis direction is 0 (a), (c) and (e) and 45 degree (b), (d) and (f) respectively.

the wave fronts). It is obvious that as layer number increases, the performance of the device gets better and approaches to the ideal case. It is also observed that the device gives similar performance for different incident angles. Actually, under the ideal case, the performance is angle independent. When the device is to be fabricated using metamaterials, the layer depth in fact is related to the size of the building blocks. From the simulation results in Fig. 6, we can conclude that the size about 1/10 wavelength can produce satisfactory results in most cases.

A transparent post is also considered and simulated when we choose $a = 0$ and $b = 0.3\,\mathrm{m}$. Under the excitation of a line source, the full-wave simulation result is shown in Fig. 7, in which the working frequency is 2 GHz, and the transformation function is chosen as $f(x) = -2(x - 0.4)^2 + 0.32$. From Fig. 7, it is very clear that the existence of the post does not affect the field distribution outside the post, while fields inside the post are changed according to (15). Though it can not be used to accommodate and protect other devices, the square-shaped transparent posts may find applications in other specific fields, such as the platform and supports of measurement systems for antennas and radar cross sections.

To quantitatively prove our arguments, we design and simulate a cylindrical transparent shell, the results are valid for other shapes too. For ease of practical implementation, a layered structure of the same size is also constructed. According to Eq. (1), the material parameter for the shell is set as follows, $\epsilon_r = \mu_r = rf'/r'$, $\epsilon_\theta = \mu_\theta = r'/(rf')$, and $\epsilon_z = \mu_z = r/(r'f')$, where $f(r)$ is the transformation function. For each layer, the parameter is chosen as that on the center circle, and totally ten layers are used in the simulation. A two-antenna array is

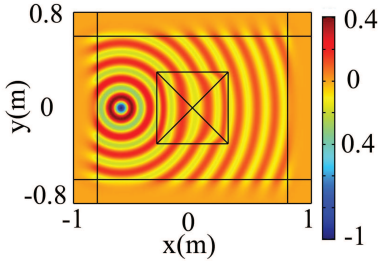

Figure 7. Electric-field distribution for the transparent post under the illumination of cylindrical waves, in which $a = 0$, $b = 0.3\,\mathrm{m}$, and the frequency is 2 GHz. The transformation function is $f(x) = -2(x - 0.4)^2 + 0.32$.

put inside the device, and simulated near field data are used to get the far field scattering pattern. The calculated results, along with the theoretical data, are shown in Fig. 8, in which the inner and outer radii of the device are 0.3 m and 0.6 m respectively, the working frequency is 2 GHz and quadratic function, i.e., $f(r) = 5/3(r-0.3)(r-0.6)+r$ is chosen for the mapping. It is clear that those data agree well with each other. Hence, our arguments on the transparent shells are once again verified. These cloaks can shield the devices inside without affecting their performances; the newly proposed devices are realizable by using artificial metamaterials; and the design method can be extended to devices with other cross sections.

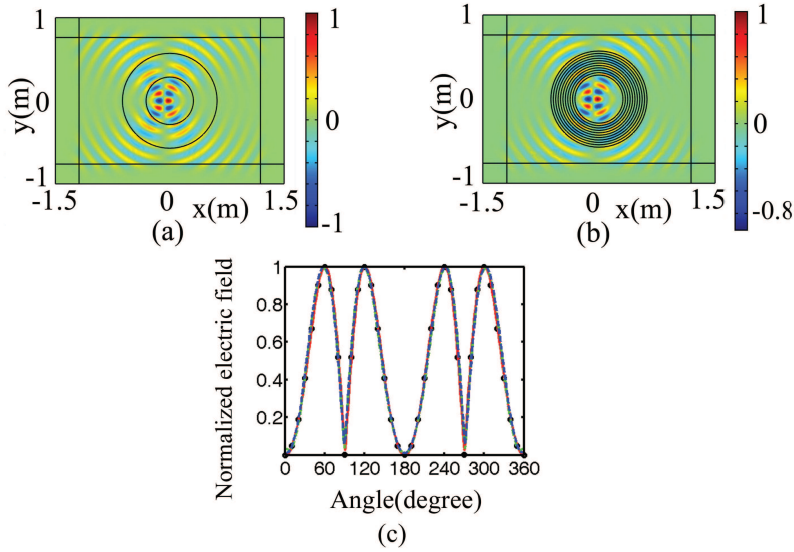

Figure 8. The normalized electric-field distribution for a two-antenna array inside an ideal (a) and a ten-layered (b) cylindrical transparent shell and the comparison for the simulated and analytical far field pattern (c). Black circle: Theoretical data; red solid line: Ideal transparent shell; green dash dotted line: Layered transparent shell without loss; blue dashed line: Layered transparent shell with loss tangent of 0.05. The analytical result is calculated with two antennae put in the free space, while the numerical one is got by using simulated near field data. Inner radius for the transparent shell $a = 0.3$ m, outer radius $b = 0.6$ m, and the working frequency is 2 GHz. The transformation function is chosen as $f(r) = 5/3(r-0.3)(r-0.6)+r$. And the two antennae are put at $(-1.5, 0)$ and $(0, 0)$ respectively with 180° phase difference.

4. CONCLUSION

In conclusion, a class of transparent shells are analyzed in this work which complement our previous study. Theoretical analysis and full-wave simulations are conducted to validate the devices. The transparent structures have wide applications in the radome structures for antennae and radar stations, in the design of materials for protecting electronic equipments, the platform and supports of measurement systems for antennae and radar cross sections, and even in the construction of anechoic rooms and concert halls.

ACKNOWLEDGMENT

This work was supported in part by a Major Project of the National Science Foundation of China (Fundamental Theories and Key Technologies of Metamaterials) under Grant No. 60990320 and 60990324, in part by the National Basic Research Program (973) of China under Grant No. 2004CB719802, in part by the Natural Science Foundation of Jiangsu Province under Grant No. BK2008031, in part by the 111 Project under Grant No. 111-2-05, and in part by the National Science Foundation of China under Grant Nos. 60871016, 60671015, and 60621002. Z. L. Mei acknowledges the support from the China Postdoctoral Science Foundation (No. 20080441006), the Inter-Discipline Science Foundation of Lanzhou University, and the Natural Science Foundation of Gansu Province (No. 0803RJZA029).

REFERENCES

1. Pendry, J. B., D. Schurig, and D. R. Smith, "Controlling electromagnetic fields," *Science*, Vol. 312, 1780–1782, 2006.
2. Schurig, D., J. J. Mock, B. J. Justice, S. A. Cummer, J. B. Pendry, A. F. Starr, and D. R. Smith, "Metamaterial electromagnetic cloak at microwave frequencies," *Science*, Vol. 314, 977–980, 2006.
3. Kwon, D. and D. H. Werner, "Restoration of antenna parameters in scattering environments using electromagnetic cloaking," *Appl. Phys. Lett.*, Vol. 92, 113507, 2008.
4. Ma, H., S. Qu, Z. Xu, and J. Wang, "The open cloak," *Appl. Phys. Lett.*, Vol. 94, 103501, 2009.
5. Kwon, D. and D. H. Werner, "Two-dimensional eccentric elliptic electromagnetic cloaks," *Appl. Phys. Lett.*, Vol. 92, 013505, 2008.
6. Mei, Z. L. and T. J. Cui, "Design of transparent cloaks with optical

transformation," *Proceedings of the 2008 International Workshop on Metamaterials*, 137–139, 2008.

7. Leonhardt, U. and T. Tyc, "Broadband invisibility by non-Euclidean cloaking," *Science*, Vol. 323, 110–112, 2009.
8. Cai, W., U. K. Chettiar, A. V. Kildishev, V. M. Shalaev, and G. W. Milton, "Nonmagnetic cloak with minimized scattering," *Appl. Phys. Lett.*, Vol. 91, 111105, 2007.
9. Rahm, M., D. Schurig, D. A. Roberts, S. A. Cummer, D. R. Smith, and J. B. Pendry, "Design of electromagnetic cloaks and concentrators using form-invariant coordinate transformations of Maxwell's equations," *Photonics Nanostruct. Fund. Appl.*, Vol. 6, 87–95, 2007.
10. Chen, H., B. I. Wu, B. Zhang, and J. A. Kong, "Electromagnetic wave interactions with a metamaterial cloak," *Phys. Rev. Lett.*, Vol. 99, 063903, 2007.
11. Cummer, S. A., B. I. Popa, D. Schurig, D. R. Smith, and J. B. Pendry, "Full-wave simulations of electromagnetic cloaking structures," *Phys. Rev. E*, Vol. 74, 036621, 2006.
12. Huang, Y., Y. Feng, and T. Jiang, "Electromagnetic cloaking by layered structure of homogeneous isotropic materials," *Opt. Express*, Vol. 15, No. 18, 11133–11141, 2007.
13. Li, J. and J. B. Pendry, "Hiding under the carpet: A new strategy for cloaking," *Phys. Rev. Lett.*, Vol. 101, 203901, 2008.
14. Liu, R., C. Ji, J. J. Mock, J. Y. Chin, T. J. Cui, and D. R. Smith, "Broadband ground-plane cloak," *Science*, Vol. 323, 366–369, 2009.
15. Lai, Y., J. Ng, H. Chen, D. Han, J. Xiao, Z. Zhang, and C. T. Chan, "Illusion optics: The optical transformation of an object into another object," *Phys. Rev. Lett.*, Vol. 102, 253902, 2009.
16. Lai, Y., H. Chen, Z. Zhang, and C. T. Chan, "Complementary media invisibility cloak that cloaks objects at a distance outside the cloaking shell," *Phys. Rev. Lett.*, Vol. 102, 093901, 2009.
17. Cai, W., U. K. Chettiar, A. V. Kildishev, and V. M. Shalaev, "Optical cloaking with metamaterials," *Nat. Photon.*, Vol. 1, 224–227, 2007.
18. Cai, W., U. K. Chettiar, A. V. Kildishev, and V. M. Shalaev, "Designs for optical cloaking with high-order transformations," *Opt. Express*, Vol. 16, No. 8, 5444–5452, 2008.
19. Valentine, J., J. Li, T. Zentgraf, G. Bartal, and X. Zhang, "An optical cloak made of dielectrics," *Nat. Materials*, Vol. 8, 568–571,

2009.

20. Gabrielli, L. H., J. Cardenas, C. B. Poitras, and M. Lipson, "Silicon nanostructure cloak operating at optical frequencies," *Nat. Photon.*, Vol. 3, 461–463, 2009.
21. Smolyaninov, I. I., V. N. Smolyaninova, A. V. Kildishev, and V. M. Shalaev, "Anisotropic metamaterials emulated by taperedwaveguides: Application to optical cloaking," *Phys. Rev. Lett.*, Vol. 102, 213901, 2009.
22. Zharova, N. A., I. V. Shadrivov, and Y. S. Kivshar, "Inside-out electromagnetic cloaking," *Opt. Express*, Vol. 16, No. 7, 4615–4620, 2008.
23. Chen, H. and C. T. Chan, "Transformation media that rotate electromagnetic fields," *Appl. Phys. Lett.*, Vol. 90, 241105, 2007.
24. Chen, H., B. Hou, S. Chen, X. Ao, W. Wen, and C. T. Chan, "Design and experimental realization of a broadband transformation media field rotator at microwave frequencies," *Phys. Rev. Lett.*, Vol. 102, 183903, 2009.
25. Tsang, M. and D. Psaltis, "Magnifying perfect lens and superlens design by coordinate transformation," *Phys. Rev. B*, Vol. 77, 035122, 2008.
26. Jiang, W. X., T. J. Cui, Q. Cheng, J. Y. Chin, X. M. Yang, R. Liu, and D. R. Smith, "Design of arbitrarily shaped concentrators based on conformally optical transformation of nonuniform rational B-spline surfaces," *Appl. Phys. Lett.*, Vol. 92, 264101, 2008.
27. Kong, F., B. I. Wu, J. A. Kong, J. Huangfu, S. Xi, and H. Chen, "Planar focusing antenna design by using coordinate transformation technology," *Appl. Phys. Lett.*, Vol. 91, 253509, 2007.
28. Jiang, W. X., T. J. Cui, X. Y. Zhou, X. M. Yang, and Q. Cheng, "Analytical design of conformally invisible cloaks for arbitrarily shaped objects," *Phys. Rev. E*, Vol. 78, 066607, 2008.
29. Schurig, D., J. B. Pendry, and D. R. Smith, "Transformation-designed optical elements," *Opt. Express*, Vol. 15, No. 22, 14772–14782, 2007.
30. Rahm, M., D. A. Roberts, J. B. Pendry, and D. R. Smith, "Transformation-optical design of adaptive beam bends and beam expanders," *Opt. Express*, Vol. 16, No. 15, 11555–11567, 2008.
31. Roberts, D. A., M. Rahm, J. B. Pendry, and D. R. Smith, "Transformation-optical design of sharp waveguide bends and corners," *Appl. Phys. Lett.*, Vol. 93, 251111, 2008.

32. Kwon, D. and D. H. Werner, "Transformation optical designs for wave collimators, flat lenses and right-angle bends," *New J. Phys.*, Vol. 10, 115023, 2008.
33. Rahm, M., S. A. Cummer, D. Schurig, J. B. Pendry, and D. R. Smith, "Optical design of reflectionless complex media by finite embedded coordinate transformations," *Phys. Rev. Lett.*, Vol. 100, 063903, 2008.
34. Tyc, T. and U. Leonhardt, "Transmutation of singularities in optical instruments," *New J. Phys.*, Vol. 10, 115038, 2008.
35. Ma, Y. G., C. K. Ong, T. Tyc, and U. Leonhardt, "An omnidirectional retroreflector based on the transmutation of dielectric singularities," *Nat. Materials*, Vol. 8, 639–642, 2009.
36. Alù, A. and N. Engheta, "Achieving transparency with plasmonic and metamaterial coatings," *Phys. Rev. E*, Vol. 72, 016623, 2005.
37. Alù, A. and N. Engheta, "Plasmonic materials in transparency and cloaking problems: Mechanism, robustness, and physical insights," *Opt. Express*, Vol. 15, 3318–3332, 2007.
38. Alù, A. and N. Engheta, "Multifrequency optical invisibility cloak with layered plasmonic shells," *Phys. Rev. Lett.*, Vol. 100, 113901, 2008.
39. Alù, A. and N. Engheta, "Cloaking a sensor," *Phys. Rev. Lett.*, Vol. 102, 233901, 2009.
40. Milton, G. W. and N. P. Nicorovici, "On the cloaking effects associated with anomalous localized resonance," *Proc. R. Soc. A*, Vol. 462, 3027–3059, 2006.
41. Vasquez, F. G., G. W. Milton, and D. Onofrei, "Broadband exterior cloaking," *Opt. Express*, Vol. 17, 14800–14805, 2009.
42. Vasquez, F. G., G. W. Milton, and D. Onofrei, "Active exterior cloaking for the 2D laplace and helmholtz equations," *Phys. Rev. Lett.*, Vol. 103, 073901, 2009.
43. Alitalo, P., O. Luukkonen, L. Jylh, J. Venermo, and S. A. Tretyakov, "Transmission-line networks cloaking objects from electromagnetic fields," *IEEE Trans. Antennas Propag.*, Vol. 56, 416–424, 2008.
44. Alitalo, P., F. Bongard, J. Zurcher, J. Mosig, and S. Tretyakov, "Experimental verification of broadband cloaking using a volumetric cloak composed of periodically stacked cylindrical transmission-line networks," *Appl. Phys. Lett.*, Vol. 94, 014103, 2009.
45. Yu, G. X., T. J. Cui, and W. X. Jiang, "Design of transparent structure using metamaterial," *J. Infrared Milli. Terahz Waves*,

Vol. 30, 633–641, 2009.

46. Leonhardt, U. and T. G. Philbin, "General relativity in electrical engineering," *New J. Phys.*, Vol. 8, 247, 2006.
47. Schurig, D., J. B. Pendry, and D. R. Smith, "Calculation of material properties and ray tracing in transformation media," *Opt. Express*, Vol. 14, No. 21, 9794–9804, 2006.
48. Milton, G. W., M. Briane, and J. R. Willis, "On cloaking for elasticity and physical equations with a transformation invariant form," *New J. Phys.*, Vol. 8, 248, 2006.